# Intentional inclusion of alkali elements Na, K in $Cu_2ZnSnSe_4$ solar cells

Sylvester Sahayaraj [2,4,5], Aniket Mule [6], Bart Vermang[3,4], Guy Brammertz[1,2], Thomas Schnabel[7], PM.P Salome[8], Marc Meuris[1,2], Jef Vleugels[5] and Jef Poortmans[2,3,4]

[1]imec division IMOMEC - partner in Solliance, Wetenschapspark 1, 3590 Diepenbeek, Belgium
[2] Institute for Material Research (IMO) Hasselt University, Wetenschapspark 1, 3590 Diepenbeek, Belgium
[3] imec- partner in Solliance, Kapeldreef 75, 3001 Leuven, Belgium
[4] Department of Electrical Engineering (ESAT), KU Leuven, Kasteelpark Arenberg 10, 3001 Heverlee, Belgium
[5] Department of Materials Engineering (MTM), KU Leuven, Kasteelpark Arenberg 44, 3001 Heverlee, Belgium
[6] Department of Mechanical and Process Engineering (D-MAVT), ETH Zurich, LEEK, Leonhardstrasse 21, 8092,
Zurich, Switzerland.
[7] Zentrum für Sonnenenergie- und Wasserstoff- Forschung Baden-Württemberg, 70565 Stuttgart, Germany

[8] International Iberian Nanotechnology Laboratory (INL), Av. Mestre José Veiga s/n, 4715-330 Braga, Portugal

**Abstract:** In this work, the addition of how much? alkali salts $Na^+$ and/or $K^+$ in the form of fluorides during the processing of $Cu_2ZnSnSe_4$ absorber layers was investigated. The difference among no, controlled and uncontrolled addition of alkali's in CZTSe has been established. The beneficial effect of alkali salts on the performance of CZTSe solar cells has been demonstrated through physical and electrical characterizations. A maximum power conversion efficiency of 8.3% has been obtained through controlled addition of both Na and K in the CZTSe absorber.

**Introduction:**

Kesterite $Cu_2ZnSn(S,Se)_4$ compounds are considered attractive potential candidates to replace the well-known Cu-based CIGS thin film photovoltaic technology due to their earth abundant constituents, low costs, low toxicity and excellent optical properties. The best efficiencies achieved for Kesterites (12.6%) [1] and CIGS (22.6%)[2] thus far have been possible with the so called "substrate architecture" where the photovoltaic absorber material is grown on top of a substrate (glass, flexible plastics, steel) followed by the deposition of other layers that make up the rest of

the solar cell. Therefore, the choice of the substrate material can be critical since it can positively or negatively influence the growth of the photovoltaic absorber. Of all choices available, the most preferred substrate is glass or more commonly soda lime glass (SLG) because it is relatively cheap, is stable over time, is corrosion resistant and can be configured in desired shapes. The composition of a typical SLG used for windows contains significant amounts of alkali elements like $Na^+$ and $K^+$ glass network modifiers [3]. The thermal properties of the glass, i.e. the strain, annealing, and glass transition point are generally between 450ºC – 720ºC, as determined by the network modifier type and content. During the growth of the photovoltaic absorber (both CZT(S,Se) and CIGS), which is typically between 450ºC – 560ºC, the glass is might go through one of these transition points (it will plastically deform above the Tg or annealing temperature) and at temperatures close to the strain point of the glass the transport properties of the constituents especially the alkali atoms are greatly enhanced enabling them to diffuse into the absorber implying the amount of alkali salts in the absorber is "uncontrolled" under these circumstances. In the case of $Cu(In,Ga)Se_2$ (CIGSe) based solar cells, the incorporation of $Na^+$ into the absorber has been reported as beneficial for the electrical performance of the devices. The importance of $Na^+$ for improved electrical performance in CIGSe was first observed in 1993 by Hedström et al. [4] and Holz et al. [5]. Since then, there have been a plethora of reports discussing several aspects related to $Na^+$ addition in CIGSe solar cells most of which can be found in [6]. As far as Kesterites are concerned, the topic of alkali element inclusion during absorber growth is still in the nascent stages of discussion. There are a few recent reports [7,8] claiming an improvement in efficiency upon $Na^+$ alkali inclusion in the kesterite absorber. In this work, a cheap and simple route to include alkali salts in a very controlled manner by spin coating in the kesterite absorber is explored and the importance of a controlled addition is discussed. The changes that take place in the absorber and eventually the solar cell upon alkali addition have been studied extensively with a variety of physical, electrical and optical techniques and an explanation accounting for these changes has been perceived. The results of solar cells with and without controlled alkali addition are compared.

## 2) Experiments and Methods

### 2.1) Sample Fabrication

The solar cells were fabricated on a 3 mm thick, 25 $cm^2$ soda lime glass (SLG) substrate covered by 400 nm of Molybdenum (Mo) as electrical back contact. The constituent elements that make up the absorber layer are deposited in a Sn(215 nm) /Zn(95 nm) /Cu (110 nm) sequence on top of the Mo-coated glass by means of electron beam evaporation. The precursor films were selenized at elevated temperatures (460ºC) in a Se-rich atmosphere created by a uniform flow of $H_2Se$ at 200 sccm in the annealing chamber to form crystalline CZTSe thin films. A temperature ramp of 1ºC/s was used and the selenization was carried out for 15 minutes before the sample was cooled down to 50ºC. In order to incorporate and systematically study the effect of $Na^+$ and $K^+$ on the performance of CZTSe solar cells, the diffusion of $Na^+$ from the SLG substrate into the CZTSe absorber was prevented. This was achieved by the use of SLG's with a 100 nm thick SiON sputtered top layer followed by the Mo layer. The alkali elements in the form of their fluorides namely NaF and KF (99.98 %, Sigma-Aldrich), were dissolved in different concentrations in DI water. Appropriate amounts of the solution was spin coated for 6 minutes on the top of the trilayer Sn/Zn/Cu metallic stack, and selenized as explained above. The selenized absorbers were then immersed in a 5 wt.% aqueous KCN/KOH solution for 120 seconds to remove secondary phases, elemental selenium and native oxides from the absorber surface. To obtain functional solar cells, a 50 nm thick CdS layer was deposited via chemical bath deposition followed by an intrinsic ZnO (120 nm) and an aluminum-doped ZnO (250 nm) layer by sputtering followed by the deposition of 50 nm of Ni and 1 µm thick Al fingers as front contact. Individual cells with an area of approximately 0.5 $cm^2$ were laterally isolated by mechanical scribing.

2.2) Physical Analysis.

The surface morphology and chemical composition of the CZGSe thin films were evaluated by scanning electron microscopy (SEM, Nova 200, FEI), equipped with an energy dispersive X-ray analysis (EDX) system. The accelerating voltage used for the EDX analysis was 20 kV. X-ray diffraction (XRD) measurements were carried out on a X'Pert Pro MRD X-ray diffractometer in the conventional Bragg-Brentano ω-2θ geometry using Cu $K_\alpha$ (1.5411 Å) radiation as incident beam. Compositional depth profiles of a wide range of elements were recorded using a Horiba Scientific GD-Profiler 2 glow discharge optical emission spectrometer (GDOES) which is operated in the RF-mode at a power of 26 W and argon pressures of 5 mbar. The measurement

spot has a diameter of 4 mm and a depth-resolution within the absorber of about 60 nm is achieved, comparable with other thin-film analytical methods like secondary ion mass spectrometry (SIMS).

2.3) Electrical and Optical Analysis.

The processed solar cells were analyzed using Current-Voltage (IV) measurements, using a 2401 Keithley Source meter, under standard test conditions for Kesterite solar cells with a solar simulator system using an AM1.5G spectrum with an illumination density of 1000 W/m2 at 25°C. The external quantum efficiency (EQE) has been measured at room temperature using a laboratory-built system with a grating monochromator-based dual-beam setup under chopped light from a Xe lamp. The doping profile of the absorbers was measured by capacitance voltage (CV) measurements, which were performed with an Agilent 4980A LCR-meter with frequencies varying from 1 kHz to 1 MHz. The excitation dependent photoluminescence analysis was measured using a Hamamatsu C12132 near infrared compact fluorescence lifetime measurement system equipped with a cryostat that can be cooled down to liquid $N_2$ (77K) temperatures. The tool uses 15 kHz, 1.2 ns pulsed 532 nm laser and the average laser power was varied between 0.08 mW to 56 mW to illuminate an area of 3 mm diameter on the measured solar cell.

## 3) Results and Discussion

### 3.1) **Effect on Physical Properties:**

Before analyzing the influence of Alkali elements in CZTSe, an appropriate concentration of each element or a combination that needs to be added to CZTSe during the absorber growth had to be sorted out. Since spin coating is a solution based technique the concentration was deduced in terms of molarity. From several selenization experiments it was observed that the carrier lifetime of CZTSe (both bare absorber and solar cells) was higher when a diffusion barrier was not used. One such example is provided in figure 1a). The minority carrier lifetimes were measured at room temperature using time resolved photoluminescence spectroscopy. The minority carrier lifetime is derived using a two exponential fit to the photoluminescence decay curve. The slower decay time is considered as the minority carrier lifetime [9]. Therefore different molar concentrations of the individual Alkali fluorides (NaF and KF) of each element and the combination (NaF + KF) starting from 0.01M to 0.5M were spin coated on top of the metallic tri layer and were selenized using the

procedure explained in the methods section. The molar concentration that gives a higher carrier lifetime than that of CZTSe absorber which has diffusion barrier for the alkalis was considered the best concentration. This screening procedure resulted in concentrations of 0.1M for both NaF and KF and 0.2M for a combination of the two which can be seen in figs.1b) -1d). This observation and screening also suggests that the presence of alkali atoms has some influence on the minority carrier lifetime of CZTSe solar cells. For the sake of simplicity and to aid better readability in the upcoming sections from now the CZTSe solar cell prepared without Na or K i.e. with a diffusion barrier will be called J-0, the CZTSe solar cell fabricated on the SLG substrate without a diffusion barrier will be called B-0. The CZTSe solar cells that have spin coated NaF will be called J-Na, spin coated KF will be called J-K, and J- Na+K , the solar cell that has both NaF and KF spin coated on the tri layer.

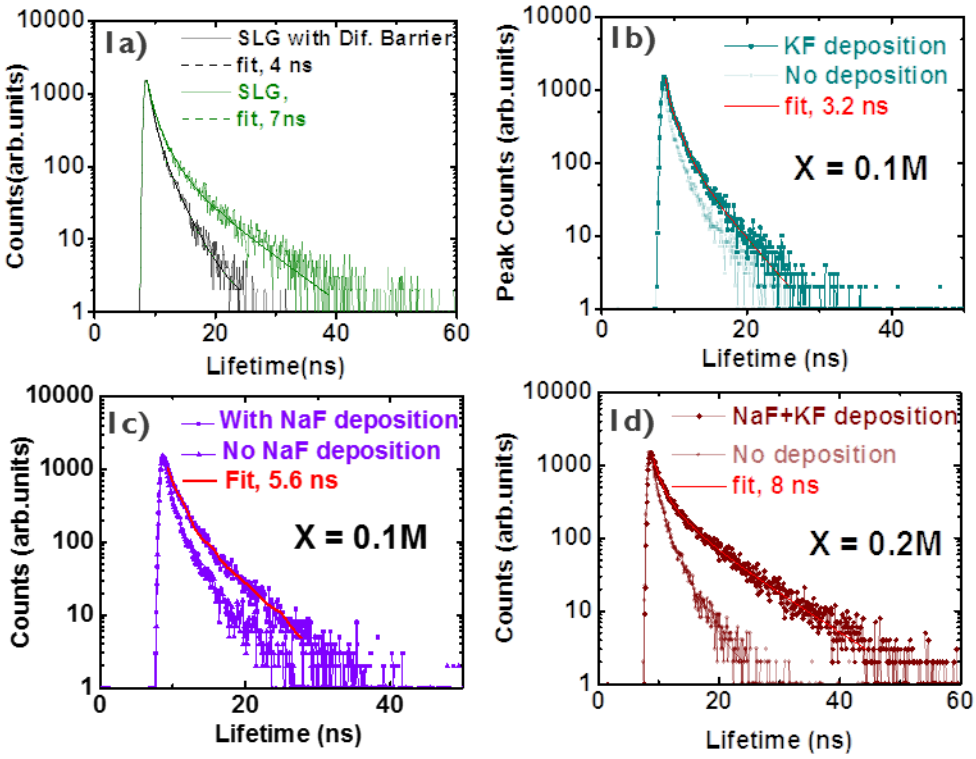


*Figure 1a) Time resolved photoluminescence measurements (TRPL) at room temperature showing the PL decay and exponential fit giving the lifetime of CZTSe solar cells with and without Na. Figures 1b) TRPL measurements of CZTSe solar cells with and without NaF external addition 1c) TRPL measurements of CZTSe solar cells with and without KF external addition 1d) TRPL measurements of CZTSe solar cells with and without NaF+ KF external addition*

The surface morphology of CZTSe absorbers B-0 and J-0 after selenization on a followed by KCN etching is shown in figs 2a) and 2b). It can be seen that the morphology of the CZTSe layers with and without Na looks quite different. In the absence of Na the shape of the grains look distinct with voids in between them compared to the absorber that has Na incorporated from the SLG substrate which has a more compact morphology. The distribution of the alkali elements Na and K in CZTSe was probed using GDOES. The measurements were performed on a full solar cell. The Glow discharge signal of the Mo back contact is plotted in order to differentiate the absorber from the remainder of the solar cell. From Fig.2c) in the sample B-0 a strong signal for Na can be detected. The measurement shows clearly that Na coming from SLG substrate during selenization is very randomly distributed in the CZTSe absorber and also tends to accumulate heavily at the backside In comparison for the J-0 sample the signal is almost 100 times weaker indicating clearly that the diffusion barrier has been quite effective in preventing the in- diffusion of Na from the substrate. The Glow discharge signal for K in both the samples is very low and almost identical . This means that either too less or no K diffuses in the CZTSe absorber during selenization.

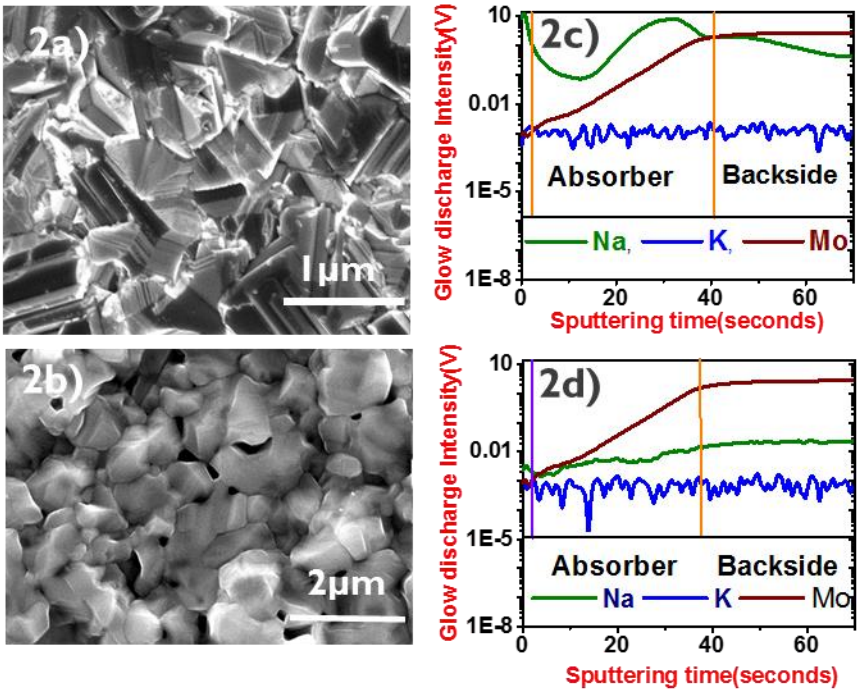


*Figure 2a) and 2b) SEM Images of the absorber in CZTSe solar cell J-0 and B-0. Figures 2c) & 2d) GDOES Elemental profiles of Na, K and Mo from CZTSe absorbers in J-0 & B-0*

The surface morphology of the CZTSe absorbers with external alkali addition i.e J-Na, J-K and J-Na+K are shown in figs. 3a) – 3c). The SEM Images present clear evidence for the considerbale improvement in morphology with controlled addition where samples J-Na and J-Na +K present big sized well defined grains. The difference in the grain sizes in the presence of alkali's especially Na can be explained by the formation of liquid phase of alkali – Se binary compounds ($Na_xSe$) during selenization. These compounds are in a liquid phase during the temperature ramp stage and can act as selenium reservoirs which can help grain growth [10,11]. The liquid alkali metal–Se binary compounds can assit quick and uniform diffusion of the constituent atoms and merge the CZTSe grain boundaries. From controlled addition of the alkali's it can be concluded that the enhanced grain growth can be attributed to the NaF top layer. In this case significant amounts of Na are readily available at the surface to react with arriving Se molecules while Na from the SLG first needs to diffuse via Mo into the CZTSe layer. The distribution of Na and K in the absorbers after controlled addition probed by GDOES is shown in Figs 3d) -3f). The glow discharge signal from Na in these samples although not as high as B-0 is still quite reasonable and higher than that of J-0. The distribution of the alkali elements is almost uniform in the absorber compared to SLG. Therefore from the data available it appears that Na is required during the absorber growth to obtain a good grain morphology but when the same is added in the right amounts as a top layer the morphology gets even better and it also results in a uniform distribution in the CZTSe absorber. However, the absorber that has only KF top layer has poorly defined grains with holes on the surface despite having a higher concentration than that of the SLG substrate.

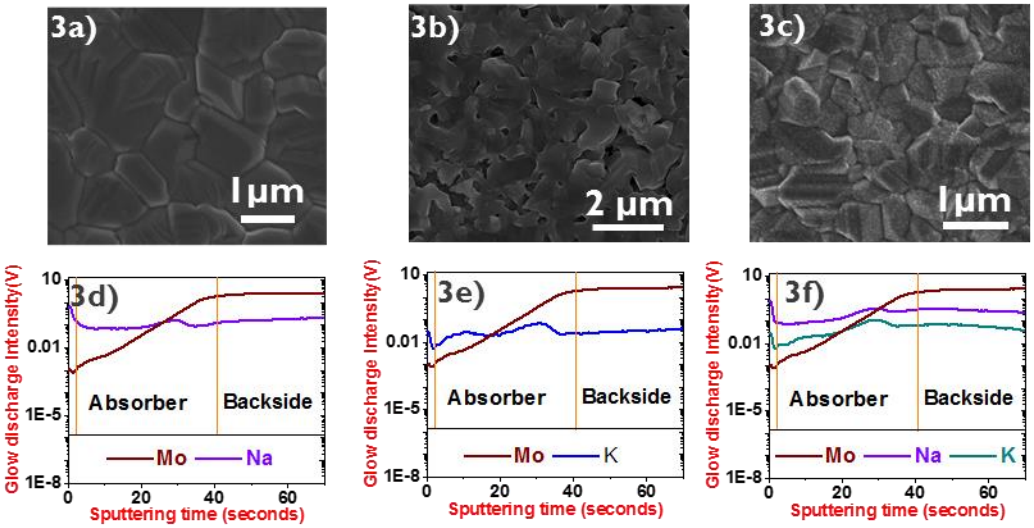


*Figure 3a) - 3c) SEM Images of the absorber in CZTSe solar cells J-Na , J-K & J- Na +K. Figures 3d) - 3f) GDOES Elemental profiles of Na, K and Mo from CZTSe absorbers in J-Na , J-K & J- Na+K*

The composition measured from these absorbers by SEM -EDX is listed in table 1 below. All the CZTSe thin films exhibit a Cu poor and Zn rich compositon. The sample J-0 has the lowest Zn/Sn ratio of all of them. When alkali salts are added not only the morphology but also the composition changes reasonably. A higher Zn/Sn ratio in the CZTSe thin films with the addition of alkali salts might suggest a possible Sn loss during the selenization which results in the higher Zn/Sn ratios. The Cu/Zn+Sn ratio is also high for these thin films which is only a consequence of lesser Sn content. This only provides information that the presence of alkali elements indeed affects the selenization reaction. How exactly this happens has not been discussed in literature so far for Kesterites and seems very tricky to speculate as well.

| Sample | Cu/Zn +Sn | Zn/Sn |
|---|---|---|
| B-0 | 0.89 | 1.15 |
| J-0 | 0.78 | 1.1 |
| J- Na | 0.86 | 1.18 |
| J-K | 0.87 | 1.19 |
| J- Na + K | 0.84 | 1.17 |

*Table 1 showing the composition of the quaternary absorber in the CZTSe solar cells with no, uncontrolled and controlled addition of Alkali elements*

In an attempt to detect the precise location of the alkali salts in the CZTSe absorber, transmission electron microsocopy (TEM) studies were performed on the cross section of 2 solar cells, J-0 and J-Na+K i.e. one solar cell without any alkali's and one with both Na and K added by spin coating. The chemical composition of the CZTSe grains was assesed by TEM-EDX mapping. From the TEM - EDX maps the presence of both Na and K could not be quantified. There are two possible reasons for this, Sodium only has one emission line Kα at 1.041 KeV. It superimposes with Zn Lα at 1.012 keV. Therefore de convolution of the siganl and further quantification could not be performed. This has been the same problem with EELS (electron energy loss spectroscopy) as

well. For K, there is a super imposition with Cd Lα. Secondly the resolution for the EDX measurements is 0.1 at %. Hence, concentrations below this limit cannot be detected either. It is certainly possible that these alkali salts are present in miniscule proportions in the CZTSe making their quantification a tough job. Therefore nothing more can be discussed about the alkali salts from the TEM studies. However, the cross sections reveal some interesting information about the CZTSe absorbers. The cross section of the J-0 solar cell is distinct from J- Na+K. The cross section (both bright and dark field images) reveal some voids similar to what was observed on the surface from the SEM images. In the vicinity of these voids some bright small sized grains can be seen. The TEM-EDX measurements reveal that these particles are particularly rich in Zn and are probably segregeates of ZnSe secondary phase. Apart from these features the composition of the absorber remains uniform across its thickness. The cross section of the J-Na+K looks quite compact and appeats to be a continuous film similar to the SEM images. At the absorber/ backside interface small aggregates are visible. From EDX measurements these aggregates were found to be very rich in Cu and Se suggesting that these particles could belong to $Cu_xSe$ secondary phase.

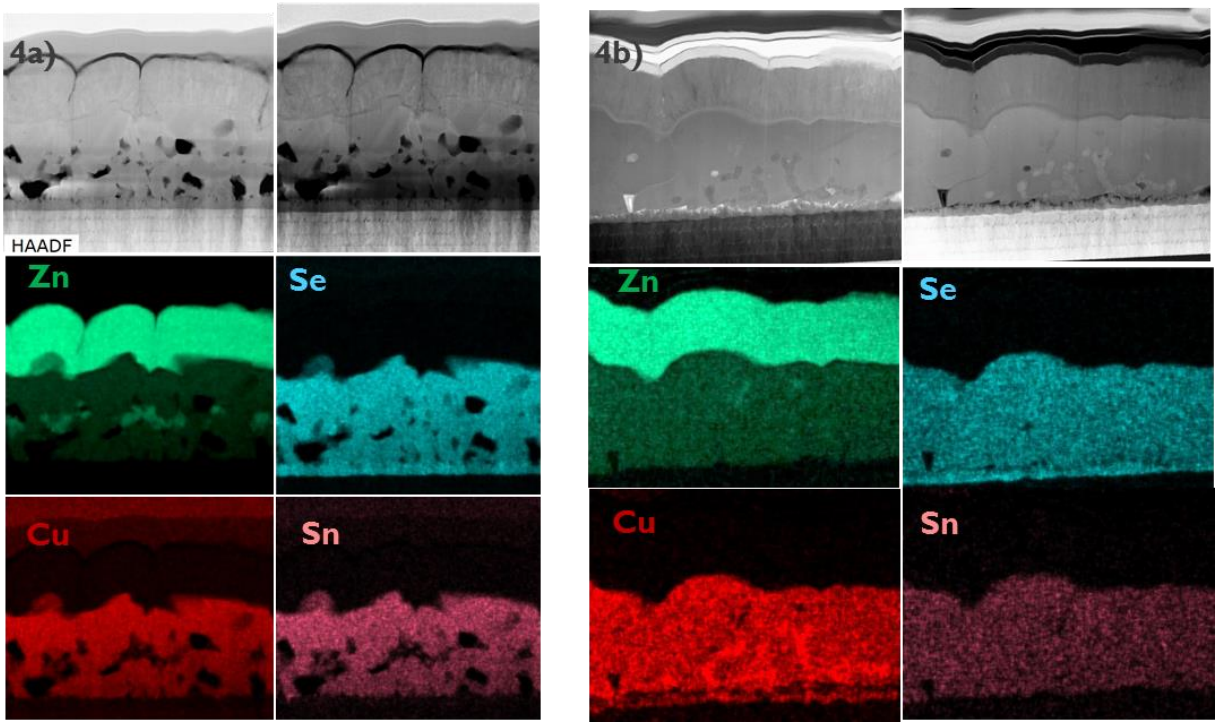


*Figure 4a) Bright and Dark FIELD TEM Images of the cross section of the CZTSe solar cell J-0(without any alkali's) along with the EDX elemental maps of the four constituent elements. Figure 4b) Bright and Dark FIELD TEM Images of the cross section of the CZTSe solar cell J- Na+ K (controlled addition by spin coating) along with the EDX elemental maps of the four constituent elements*

XRD measurments performed on these absorbers also share similar information. The XRD pattern of the solar cells is shown in Fig 5a). The major diffraction peaks can be indexed to the Tetragonal CZTSe phase. The other secondary phases in the XRD pattern are indexed using PDF cards listed in [30]. The zoomed in section of the main (112) peak shown in Fig 5b) shows that the CZTSe absorbers with alkali inclusion is shifted to the lower theta whereas for the absorber without alkali the main peak stays exactly at 27.16º. A shift to lower diffraction angles can be due to several reasons but the most likely and convincing of them all is an increase in the lattice constant. This can happen due to alkali atoms occupying some positions in the unit cell of CZTSe or by substituting one of the constituent elements of CZTSe. The extent of this shift does not seem to depend on the size of the alkali atoms. The sample B-0 where Na is incorporated in uncontrolled fashion exhibits a larger shift in the 2Θ. From GDOES it was observed that the Na distribution in the absorber is higher in comparison with controlled addition. Therefore the extent of this shift should be related to the amount of the alkali atoms available for incorporation rather than the kind of the alkali atom. To add more support to the TEM data the zoomed in section of the XRD pattern shown in Fig.5c) shows the presence of CuSe secondary phase in small proportion in the samples J-Na+K, J-Na and B-0 all of which contain Na. Sn related secondary phases (SnSe, $SnSe_2$) were seen in the solar cells J-Na and J-K but not in the others. Since the XRD measurements were performed on the solar cells, peaks of ZnO are also seen in the XRD pattern. The combined information from, TEM -EDX and XRD anlaysis indicates the presence and precise location of different secondary phases in the solar cells with and without alkali elements clearly. Although an hypothesis explaining this difference cannot be derived from this data alone.

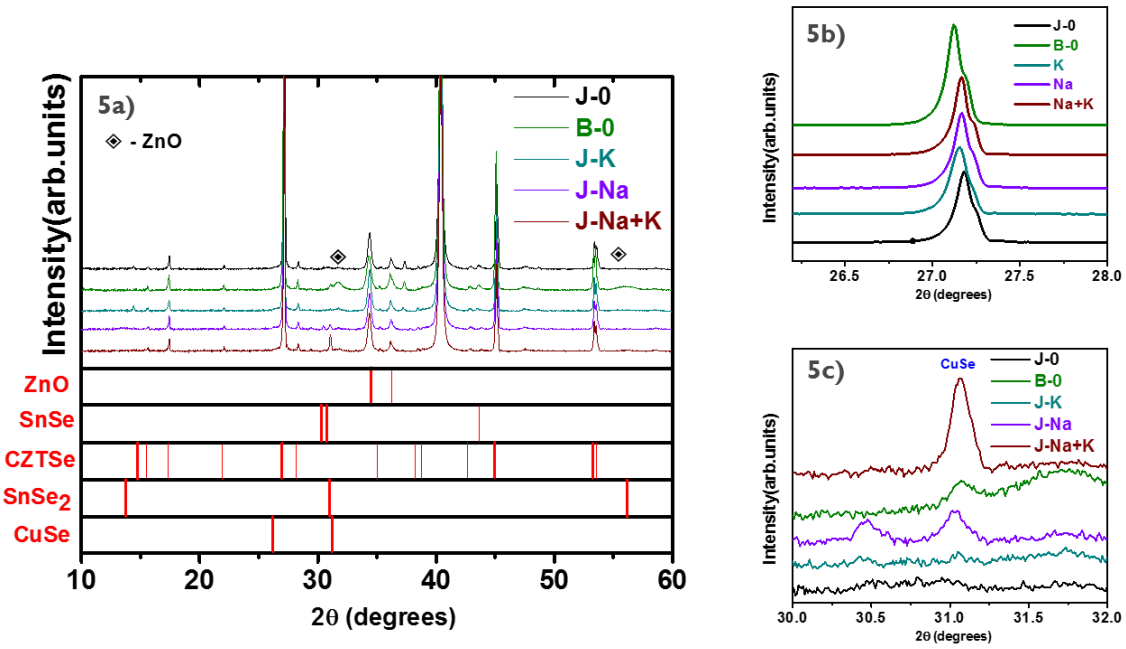


*Figure 5a) X Ray Diffraction pattern of the CZTSe solar cells with no, uncontrolled and controlled addition of Alkali elements. Figure 5b) Section of the XRD pattern showing the main (112) peak of all the CZTSe solar cells. 5c) Section of the XRD pattern showing the different secondary phases in all the CZTSe solar cells.*

### 3.2) Effect on Electrical and Optical Properties

The solar cell parameters of the devices in discussion are listed in the table below. The IV curves of the best cells are plotted in the figure 6a) , the average and standard deviation measured from 12 functional cells along with other solar cell parameters for each device is shown in table 2 below. It can be clearly seen that the efficiency of the solar cell without any alkali's is lower than the rest. The solar cell which has controlled addition of Na or both Na + K is considerably higher whereas the efficiency of the cell which has Na incorporation through uncontrolled addition has a moderate value between the two. The open circuit voltage $V_{oc}$ of all solar cells which contain alkali salts are also significantly higher than the solar cell without the alkali's (J-0). The improvement in the solar cell efficiency with alkali incorporation is also due to a noticeable increase in the short circuit density ($J_{sc}$). The spectral response measurements shown in figure 6b) justify this statement. The carrier collection in all the the solar cells is very uniform up to 400 nm, which corresponds to the parastic absorption region of the TCO's. In the range 500 nm – 1000 nm,

(visible to far infra red) the solar cells J-Na, J-Na+K i.e solar cells with controlled alkali addition show a remarkable increase in the carrier collection efficiency which exceeds 90%. One possibility that could explain this response can be the continuous well defined surface morphology of the CZTSe absorbers in these solar cells. A similar Jsc increase that comes from the improvement of long wavelength collection was also reported by Gershon et al., in their Na incorporation studies in CZTSe. From the defect analysis they performed they were able to realize when the subgap states are shallower, the carrier mobility and hence longwavelength collection efficiency improved [12]. The same could be true here although no experimental data is available to prove this. The response of the other solar cells in this region is only moderate in comparison. As a result of this excellent carrier collection the solar cells short circuit current densities of J-Na and J-Na+K measured from EQE turn out to be 37 and 38 mA/cm$^2$ respectively as opposed to 31.4 mA/cm$^2$ for J-0 and 30.2 cm$^2$ for B-0.

| Sample code | $J_{sc}$ (mA/cm$^2$) | $V_{oc}$ (mV) | FF | Eff. η% |
|---|---|---|---|---|
| J-0 | 31.6 | 330 | 50.8 | 5.3% (4.7±0.6)% |
| B-0 | 30 | 415 | 53.6 | 6.7% (6.3±0.4)% |
| J-K | 28.1 | 364 | 51 | 5.4% (4.7±0.7)% |
| J-Na | 35 | 409 | 54 | 7.9% (7.5±0.4)% |
| J- Na +K | 36.2 | 421 | 53 | 8.3 % (7.8±0.5)% |

*Table 2 showing the IV parameters(AM 1.5G) of the CZTSe solar cells with no, uncontrolled and controlled addition of Alkali elements*

Figure 6c) shows the carrier density profiles of a set of CZTSe solar cells processed at different times, with and without the diffusion barrier from CV measurements. From the figure it is very evident that the carrier density of CZTSe solar cells without the diffusion barrier (B-0, B-0', B-0") is consistently higher than their counterparts. The carrier density is about 10 times higher when Na is incorporated in CZTSe. The increase in carrier density is accompanied by a change in the Fermi level. When all devices have the same kind of processing, except for the absorber everything else remains the same. Therefore the fermi level changes only in the p type absorber. This change of

bulk Fermi level will affect the built in potential ($V_{bi}$) of the p-n junction. The built in potential extracted by Mott - Schottky plots for devices J-0 and B-0 are shown in Figs. 6d) and 6e). The built in potential with Na incorporation is higher by 100 mV. A higher built-in voltage may lead to higher $V_{oc}$ because the built-in voltage is the upper limit of $V_{oc}$. Indeed, the $V_{oc}$ of B-0 device is 85 mV higher than that of J-0 device. The exact mechanism on how the change in carrier density happens with Na is not clearly known for Kesterites. All that is experimentally known in this case is that with Na inclusion the p-type carrier density increases. Niles et al. encountered the exact situation in CIGS. From XPS analysis they were able to conclude when Na is present during CIGS growth it was replacing either In or Ga in order to form acceptor states that resulted in higher p-type carrier concentration [13]. It is well known that CZTSe is a derivative of CIGS where In and Ga are replaced by Zn and Sn. Now if Na replaces Cu in CZTSe it would lead to the formation of $Na_{Cu}$ defects that will not create acceptor states, because Na and Cu are both column I elements. Na replacing Se would result in an all metallic compound which will diminish the semiconductor behavior of the solar cell. Since Zn and Sn are present in 2+ and 4+ states in CZTSe, Na occupying either a Zn or a Sn site would result in acceptor states such as $Na_{Zn}$ or $Na_{Sn}$. The formation energy of compensated defect clusters is much lower and more favorable than that of single donors or acceptors in CZTSe due to charge transfer and attractive Coulomb interaction between the atoms[14]. The formation of $Na_{Sn}$ is feasible but such defects would result in triple acceptor states which require a triple donor state like $Sn_{Cu}$ for compensation, the formation of which is possible only in Cu rich Kesterites. Therefore in Cu poor Kesterites the most likely explanation for the increase in the carrier density with Na incorporation stems from the formation of $Na_{Zn}$ acceptor defects. This hypothesis is also supported by XRD measurements which show the main CZTSe peaks are shifted to smaller theta that reflects an increase in lattice constant due to alkali doping.

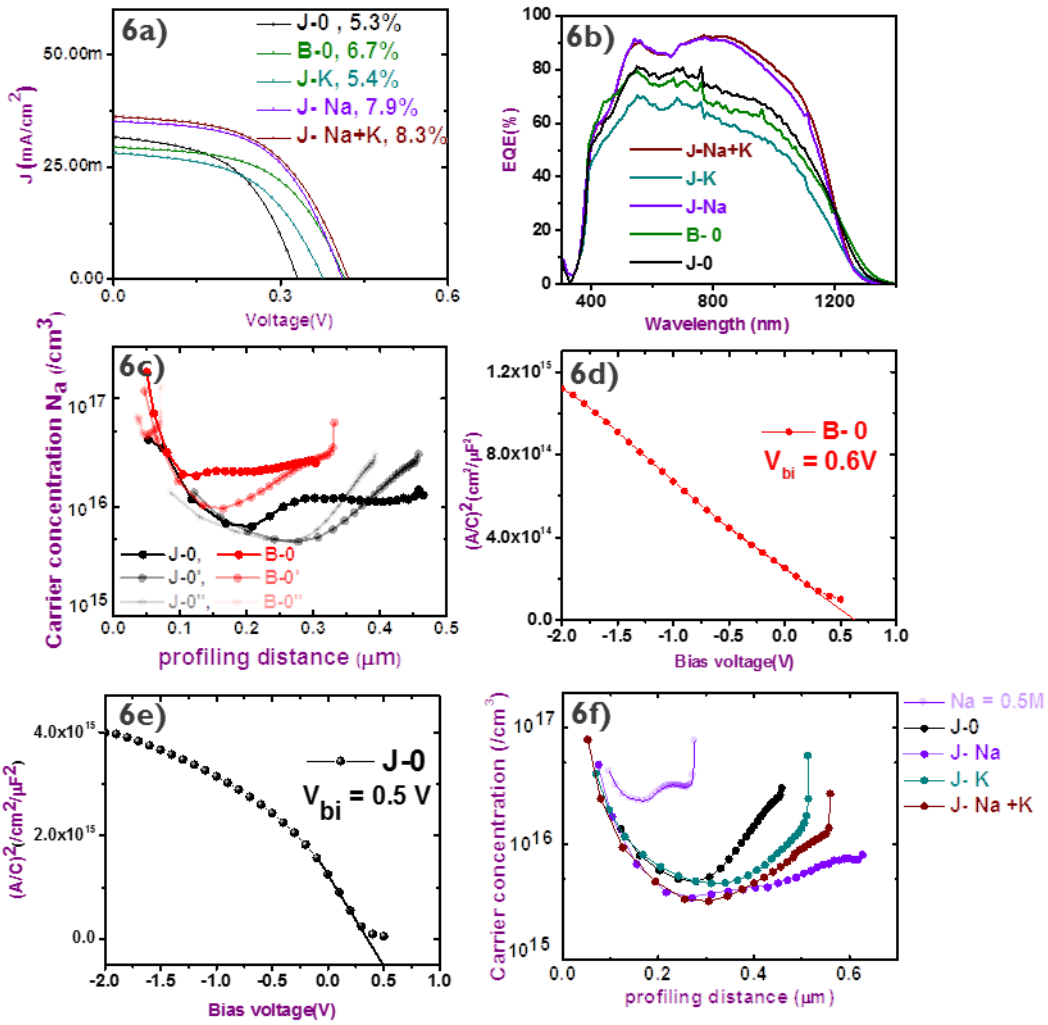


*Figure 6a) Illuminated IV curves of the best CZTSe cells with no , uncontrolled and controlled alkali addition. Figure 6b) External Quantum efficiency (EQE) curves of the best CZTSe cells with no, uncontrolled and controlled alkali addition. Figure 6c) Carrier density profiles obtained from CV measurements for a set of CZTSe solar cells with no and uncontrolled alkali addition. Figures 6d) and 6e) Mott- Schottky plots to extract the Built in voltage ($V_{bi}$) of CZTSe solar cells with no and uncontrolled Na addition. Figure 6f) Carrier density profiles obtained from CV measurements for a set of CZTSe solar cells with controlled alkali addition.*

The change in net carrier density with controlled alkali addition is shown in fig.6f). With controlled addition there is very less change in the carrier density. In fact the carrier density is lowered in the absorber when only 0.1M and 0.2M concentrations of alkali salts are used. The depletion width is also higher in the case of controlled addition comparatively. From the previous section it was seen that although controlled addition results in a uniform distribution of alkali salts in the CZTSe absorber the amount of alkali's incorporated in the absorber is lesser compared to the in diffusion

of Na from the SLG and it is very likely to be below 0.1at%. Therefore with these low amounts the effect on carrier density is not the same as what was observed with uncontrolled addition. However, when 0.5M of Na is added through controlled addition the carrier density curve resembles that of the B-0's. Therefore by tailoring the amount of alkali salts in CZTSe during the absorber formation the p type doping can be modified. The optimum carrier density for high efficient devices seems to be around the $10^{15}/cm^3$ mark. Another point of interest is that the built in potential ($V_{bi}$) of the devices with controlled addition is very similar to that of J-0 but the $V_{oc}$ of these devices is significantly higher than J-0. This shows that besides the limitation of the built in voltage there are certainly other reasons for the Voc enhancement. In order to understand some of those, in depth optical and electrical analysis were performed on the CZTSe solar cells used in this discussion. Firstly excitation dependent photoluminescence was performed. The recombination mechanism explained by the Quasi Donor to Acceptor transitions (Q-DAP) is the best model for these devices (except for J-K). The concepts, equations that explain the Q-DAP model from Gershon et al. [15] have also been employed successfully to understand both S and Se based Kesterites [15-17]. A useful quantity that can be measured from the excitation dependent analysis is the Q - DAP pair density in other words the density of charge compensating defect clusters in the absorber. The calculated defect density has been plotted against the $V_{oc}$ of the solar cells in fig.7a) and the power conversion efficiency of the solar cells in fig.7b). Both the efficiency and the $V_{oc}$ of the solar cell trend linearly with the Q-DAP defect density of the absorbers. A higher defect density was seen to correlate with a low $V_{oc}$ and lower efficiency and vice versa. A higher Q-DAP defect density was seen in the device J-0 without any alkali's. The defect density in the devices with alkali (either controlled or uncontrolled) differ by an order of magnitude compared to J-0 and this also reflects in the $V_{oc}$ of these devices which are significantly higher than J-0. Large defect densities and heavy compensation can reduce the $V_{oc}$, e.g., by the formation of band tail states [18] in as much as defects may participate in trapping and recombination processes.[19–21]. The fact that devices containing alkali's exhibit a higher $V_{oc}$ means the presence of alkali atoms certainly mitigates the recombination losses e.g., by passivating some defects, in the absorber to an extent. At this juncture it is worth recollecting the observation made earlier in this discussion where the minority carrier lifetime of the CZTSe solar cells was always higher with Na inclusion. Combining these ideas it is easy to see that a higher bulk defect density, low lifetimes, low $V_{oc}$ and ultimately a lower power conversion efficiency turn out to be characteristics of alkali

free CZTSe solar cells. The converse of this holds fine indeed. The behavior of the $V_{oc}$ with temperature obtained from temperature dependent IV measurements is shown in Fig 7c). The extrapolation of the $V_{oc}$ at 0K usually is interpreted as giving the activation energy of the dominant recombination process in the solar cell [22]. It can be seen that the extrapolated $V_{oc}$ at 0K for all devices is lower than the value of $E_g/q$ (1.05V, the actual band gap of CZTSe) which seems to indicate that the $V_{oc}$ is limited by recombination at the absorber – buffer interface similar to most Kesterite devices. Particularly the device J-0, has a very low $V_{oc}$ max. or in other words a large $V_{oc}$ deficit. This also indicates a high density of interface defect states in alkali free CZTSe devices.

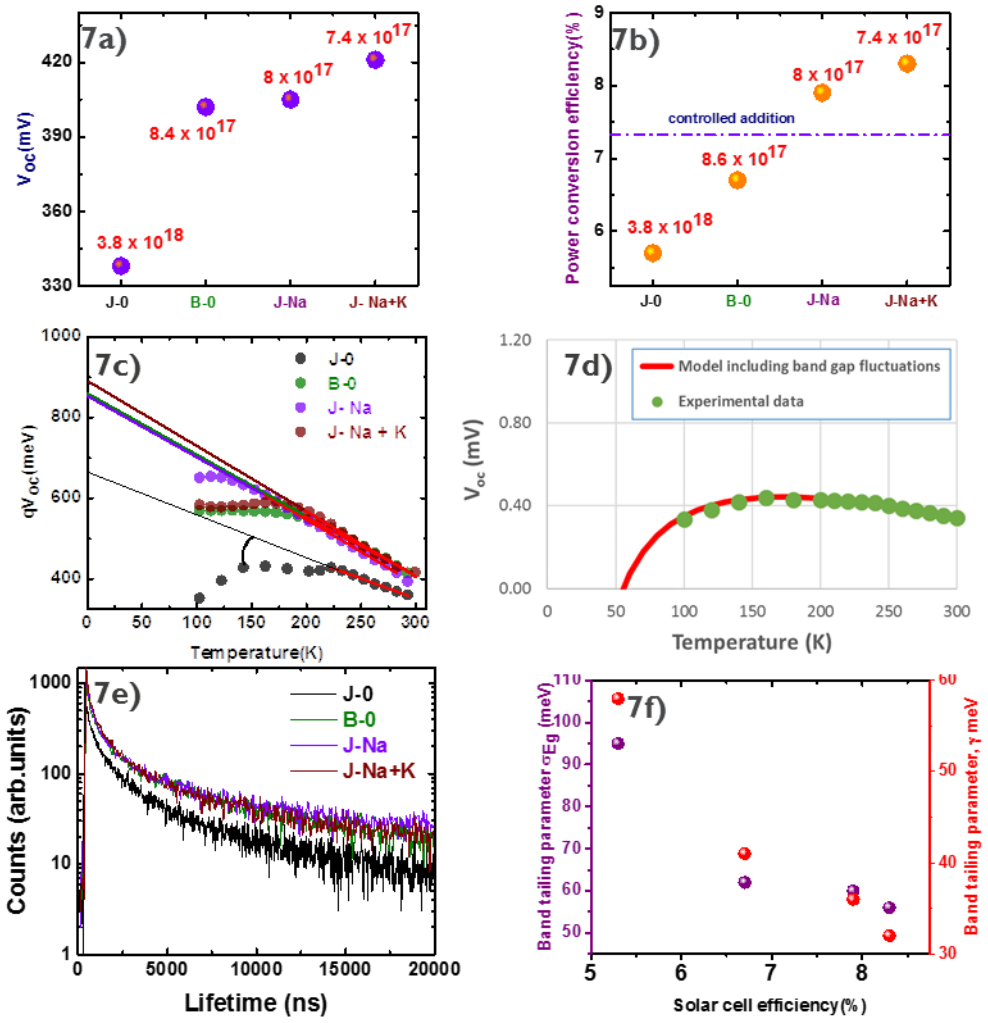


*Figure 7a) Plot showing the relation between the bulk Q-DAP defect density and the open circuit voltage the CZTSe cells with no , uncontrolled and controlled alkali addition. Figure 7b) Plot showing the relation between the bulk Q-DAP defect density and the efficiencies of the same. Figure 7c) Behavior of the Voc with temperature deduced from low temperature IV measurements in CZTSe solar cells with no, uncontrolled and controlled alkali addition. Figures 7d) An example plot explaining the extraction of the band tailing parameter σ from low temperature IV measurements. 7e) Time resolved photoluminescence spectra showing enhanced lifetimes at 77K. Figure 7f) Band tailing parameters (σ & Γ) versus the efficiency of the solar cells with no , uncontrolled and controlled alkali addition.*

A characteristic feature of Kesterite solar cells is the presence of absorption tails at the band edges which can act as centers of non-radiative recombination. This band tailing in CZTSe can arise due to the existence of spatial band gap fluctuations that arise due to differences in the composition or secondary phases or electrostatic potential fluctuations (presence of a band gap with parallel shifts in valence and conduction band edges) that arise due to defect clustering or uncompensated charge complexes in the absorber. Both cases lead to a non-zero density of states within the band gap. The fundamental difference between band tailing caused by spatial band gap fluctuations and potential fluctuations at the microscopic level is shown in figure 8a) and 8b) (figure adapted from [23]).

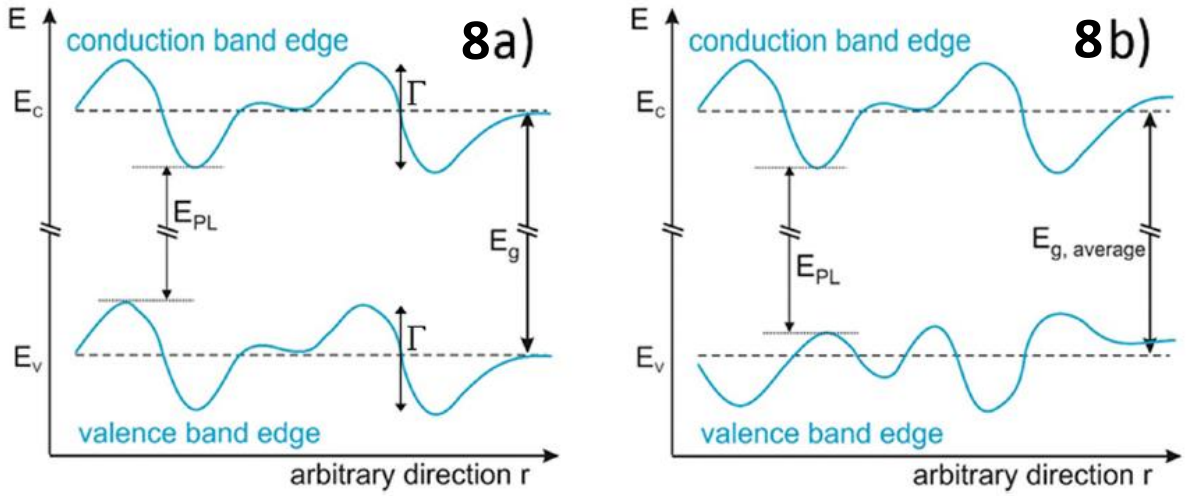


The roll over effect of the $V_{oc}$ observed in the low temperature regime is usually related to spatial band gap fluctuations. From fig.7c) it is evident that all the solar cells used in this discussion suffer from these band gap fluctuations. An alternative interpretation to the data shown in Fig.7c) could be given by fitting the data with the equation derived by Rau et al., for a photovoltaic absorber presenting spatial or lateral band gap fluctuations [24]. Taking the

$$V_{OC} = \frac{\overline{E_g}}{q} - \frac{\sigma_{E_g}^2}{2kTq} - \frac{kT}{q}\log\left(\frac{J_{00}}{J_{SC}}\right)$$

A good fit to the experimental data can be obtained using the equation shown above, using as fitting parameters the activation energy of the dominant recombination process equal to the band gap value 1.05 eV and a magnitude of the band gap fluctuations ($\sigma_{Eg}$) for each $V_{oc}$ curve. Figure 7c) could therefore also be interpreted in a way that the dominant recombination process is in the bulk of the absorber and not at the interface and that the intersect with zero Kelvin is reduced because of the presence of a relatively large amount of band gap fluctuations in the absorber which is very severe in the device J-0. The $\sigma_{Eg}$ values have been quantified and listed below in table 3.

| Sample | $\sigma_{Eg}$ VALUE |
|---|---|
| J- Na +K | 60 |
| J-Na | 50 |
| B – 0 | 62 |
| J-0 | 94 |

*Table 3 showing the band tailing parameter σ derived from the equation from Rau et al., in the CZTSe solar cells*

Previously from photoluminescence measurements the presence of bulk defect complexes and their densities in the CZTSe absorbers was established. This gives rise to electrostatic potential fluctuations in the absorber. The extent of the band tailing due to the electrostatic fluctuations in the absorber can be quantified from the Γ parameter that can be calculated from Low temperature PL analysis using the formula given in [25]. The values of $\sigma_{Eg}$ and Γ for the CZTSe solar cells in this discussion have been calculated and are plotted against the efficiency of the cells. Both band gap and potential fluctuations have the same effect on recombination in the absorber but they are fundamentally different on the microscopic level. In order to distinguish both and figure out which mechanism results in band tailing in these solar cells time resolved photoluminescence measurements were carried out at 77K. The outcome of these measurements in the solar cells is shown in Fig 7e) where enhanced lifetimes are observed in all the cases. The long lifetimes are a

consequence of electro static potential fluctuations which separates the charge carriers spatially. The explanation behind these enhanced lifetimes is provided by Gokemon et al., [18] which can also be adapted for CZTSe solar cells used in this discussion. The Γ parameter, the average potential fluctuation calculated from PL measurements is shown in Fig 7f) versus the efficiency of the solar cell. Once again, J-0 has a higher value (60 meV) than the remaining solar cells which contain alkali salts. Γ increases with increasing density of compensating donors and acceptors [26,27,28]. This is also true in this case where a Q-DAP defect density of the order of $10^{18}/cm^3$ was observed in the sample J-0 which is higher than the other CZTSe solar cells leading to a higher degree of band tailing resulting in higher recombination losses. These findings clearly prove that Na or K in CZTSe modifies the degree of compensation in the absorber in a beneficial manner. The solar cells with controlled addition of alkali salts show lesser degree of band tailing and lower density of compensating defects which are likely reasons for their high $V_{oc}$. Nevertheless the efficiencies obtained through the controlled addition experiment are still lower than the record efficiencies of Kesterites. This is probably due to the presence of secondary phases (CuSe, SnSe) in the thin film along with CZTSe. Both these phases are known to reduce the $V_{oc}$ and the shunt resistance (the FF indirectly) [29] thereby limiting the efficiencies.

## Summary.

A concise account of the effect of the alkali atoms (Na and K) on the physical, electrical and optical properties of CZTSe solar cells has been presented. The presence of alkali atoms looks certainly beneficial for CZTSe solar cells. The inclusion of Na in CZTSe from the soda lime glass substrate and by controlled spin coating experiment was discussed. Na from SLG enters CZTSe from the backside through Mo in an uncontrolled way. The amount of K diffusion is either too little or nothing to have any impact on the performance of CZTSe. When both Na and K are added in right amounts as NaF and KF top layers the morphology of CZTSe grains improve considerably and the distribution of these elements in the CZTSe absorber is also very homogeneous. The controlled addition of both Na and K also results in high efficient CZTSe devices reaching efficiencies up to 8.3% as opposed to 6.7% for uncontrolled addition. The open circuit voltage in both cases was very much the same in both cases but the devices with controlled addition show lesser p- type doping, a low density of charged defects and less band tailing compared to the rest. These

experiments and findings illustrate not only the importance of alkali salts in the processing of CZTSe solar cells but also the impact of controlled addition on their properties.

**Acknowledgements:**

This research is partially funded by the Flemish government, Department Economy, Science and innovation. This research has received funding from the European Union's Horizon 2020 research and innovation program under grant agreement No 640868.

**References:**

[1] J. Kim, H. Hiroi, T. Todorov, T.O. Gunawan, M. Kuwahara, T. Gokmen, D. Nair, M. Hopstaken, B. Shin, Y.S. Lee, W. Wang, H. Sugimoto, D.B. Mitzi, Adv. Mater. 26, 7427 (2014).

[2] www.pv-tech.org/news/zsw-Achieves-World-Record-Cigs-Lab-Cell-Efficiency-of-22.6.

[3] www.menzel.de/on2014/07/16.

[4] J.Hedström,H.Ohlsen,M.Bodegård,A.Kylner,L.Stolt,ZnO/CdS/Cu(In,Ga)Se2 thin film solar cells with improved performance in: Proceedings of the 23rd IEEE Photovoltaic Specialists Conference,1993, pp.364–371.

[5] J.Holz, F.Karg, H.von Philipsborn, The effect of substrate impurities on the electronic conductivity in CIS thin films, Presented at the12th European Photovoltaic Solar Energy Conference, Amsterdam, Netherlands,1994, p.1592.

[6] Incorporation of alkali metals in chalcogenide solar cells, P.M.P. Salomé H. Rodriguez-Alvarez, S. Sadewasser. Solar Energy Materials & Solar Cells,143 (2015), 9–20.

[7] Influence of alkali metals (Na, Li, Rb) on the performance of electrostatic spray-assisted vapor deposited $Cu_2ZnSn(S,Se)_4$ solar cells. Giovanni Altamura, Ming qing Wang & Kwang-Leong Choy, Scientific reports, 6:22109.

[8] Efficiency Enhancement of $Cu_2$ $ZnSn(S,Se)_4$ Solar Cells via Alkali Metals Doping, Yao-Tsung Hsieh , Qifeng Han , Cheng yang Jiang , Tze-Bin Song , Huajun Chen , Lei Meng , Huan ping Zhou and Yang Yang. Adv. Energy Mater. 2016, 6, 1502386.

[9] A. Kanevce, D.H. Levi, D. Kuciauskas, Prog. Photovolt.: 23 Res. Appl. 22, 1138 (2014).

[10] J. Sangster , A. D. Pelton , J. Phase Equilib. 1997 , 18 , 177

[11] D. Braunger , D. Hariskos , G. Bilger , U. Rau , H. W. Schock , Thin Solid Films 2000 , 361–362 , 161 .

[12] The impact of sodium on the sub-bandgap states in CZTSe and CZTS .Talia Gershon, Yun Seog Lee, Ravin Mankad, Oki Gunawan, Tayfun Gokmen, Doug Bishop, Brian McCandless, and Supratik Guha APP. Phy. LETTERS 106, 123905 (2015).

[13] Na impurity chemistry in photovoltaic CIGS thin films: Investigation with x-ray photoelectron spectroscopy. David W. Niles, Kannan Ramanathan, Falah Hasoon, Rommel Noufi, Brian J. Tielsch, and Julia E. Fulghum. J. Vac. Sci. Technol. A 15„ 6…, Nov/Dec 1997.

[14] S. Chen, J. H. Yang, X. G. Gong, A. Walsh, and S. H. Wei, Phys. Rev. B 81, 245204 (2010).

[15] T. Gershon, B. Shin, N. Bojarczuk, T.Gokmen, S.Lu, and S. Guha, Photoluminescence characterization of a high-efficiency $Cu_2ZnSnS_4$ device. Journal of Applied Physics **114**, (2013), 154905.

[16] Effect of the duration of a wet KCN etching step and post deposition annealing on the efficiency of $Cu_2ZnSnSe_4$ solar cells. Thin Solid Films (2016), http://dx.doi.org/10.1016/j.tsf.2016.09.055

[17] Sahayaraj et al., " Optoelectronic properties of CZGSe thin film solar cells" – Article submitted to "Solar Energy Materials and Solar cells"

[18] T. Gokmen, O. Gunawan, T. K. Todorov, and D. B. Mitzi, Appl. Phys.Lett. 103, 103506 (2013).

[19] D. Macdonald and A. Cuevas, Prog. Photovoltaics 8, 363 (2000).

[20] I. Repins, M. A. Contreras, B. Egaas, C. DeHart, J. Scharf, C. L. Perkins, B. To, and R. Noufi, Prog. Photovoltaics 16, 235 (2008).

[21] A. J. Lochtefeld, M. R. Melloch, J. C. P. Chang, and E. S. Harmon, Appl.Phys. Lett. 69, 1465 (1996).

[22] Scheer, R. & Schock, H. W. Chalcogenide Photovoltaics (2011). Wiley-VCH Verlag Gmbh & Co, KGaA, Weinheim.

[23] Bourdais et al., Adv. Energy Mater. 2016, 6, 1502276

[24] U. Rau and J. H. Werner, "Radiative efficiency limits of solar cells with lateral band-gap fluctuations", App. Phy. letters, 84, (2004),3735.

[25] B.I Shklovskii, and A.L. Efros, Electronic Properties of Doped Semiconductors, (1984) Springer, Berlin.

[26] V. Dobrego , I. Shlimak , Phys. Stat. Sol. B. 1969 , 33 , 805 ;

[27] Z. I. Alferov , V. M. Andreev , D. Z. Garbuzov , M. K. Trukan , Soviet Physics – Semicond. 1973 , 6, 1718

[28] P. W. Yu , J. Appl. Phys. 1977 , 48 , 5043.

[29] Sylvester Sahayaraj, Guy Brammertz, Marie Buffi`ere, Marc Meuris, Jef Vleugels, Jef Poortmans, "Effect of Cu content and temperature on the properties of Cu2ZnSnSe4 solar cells", EPJ Photovoltaics 7, 70304 (2016).

[30] International Center for Diffraction Data: CZTSe – 04- 010-6295; MoSe2 – 04-004-8782; SnSe: 04-009-2274; $SnSe_2$:01-089-2939; ZnSe: 04-015-0312; CuSe: 00-049-1456; Mo:01-088-331.

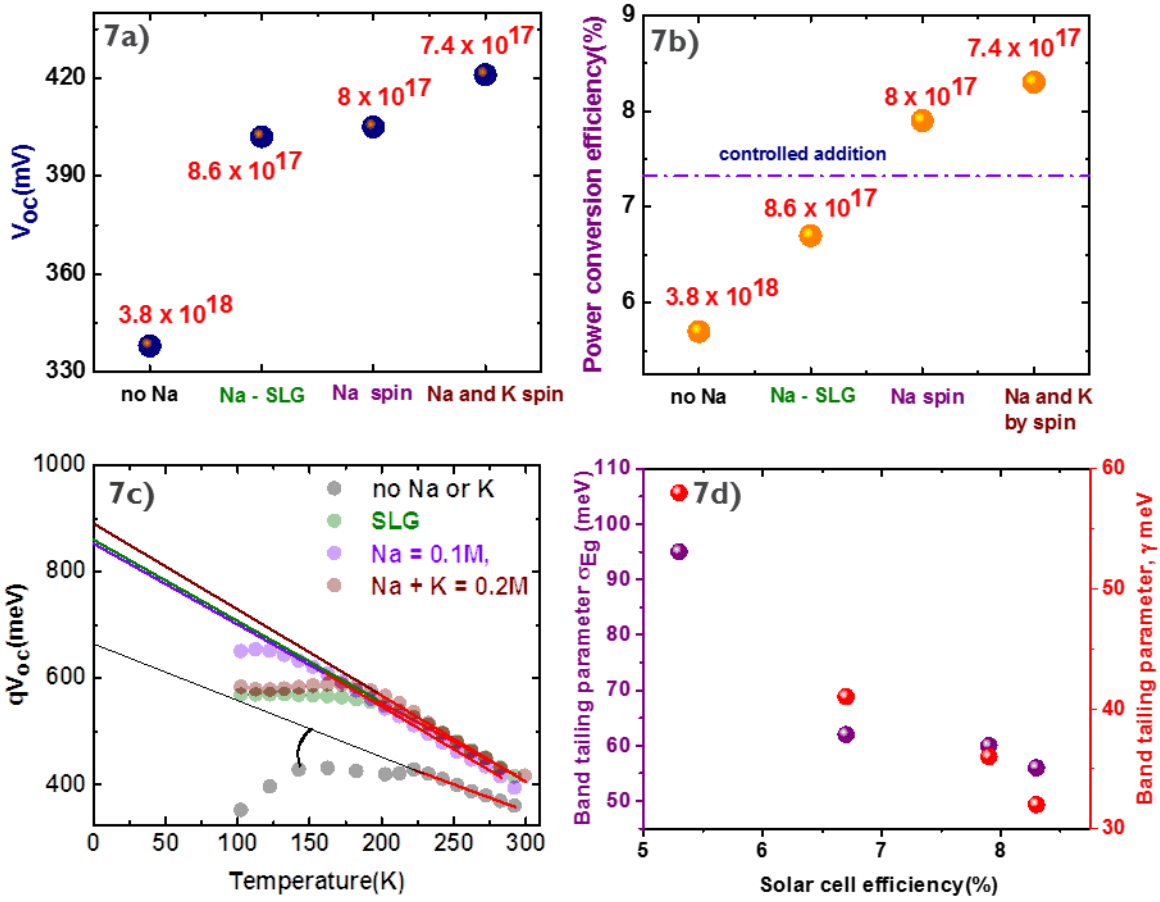
7a)
$V_{oc}$(mV)
420
390
360
330
7.4 x $10^{17}$
8 x $10^{17}$
8.6 x $10^{17}$
3.8 x $10^{18}$
no Na
Na - SLG
Na spin
Na and K spin
7b)
Power conversion efficiency(%)
9
8
7
6
7.4 x $10^{17}$
8 x $10^{17}$
controlled addition
8.6 x $10^{17}$
3.8 x $10^{18}$
no Na
Na - SLG
Na spin
Na and K by spin
7c)
$qV_{oc}$(meV)
1000
800
600
400
no Na or K
SLG
Na = 0.1M,
Na + K = 0.2M
0
50
100
150
200
250
300
Temperature(K)
7d)
Band tailing parameter $\sigma_{Eg}$ (meV)
110
100
90
80
70
60
50
Band tailing parameter, γ meV
60
50
40
30
5
6
7
8
Solar cell efficiency(%)